Confined Water Dissociation in Microporous Defective Silicates: Mechanism, Dipole Distribution, and Impact on Substrate Properties

Hegoi Manzano,*,[‡],[†] Sina Moeini,[‡] Francis Marinelli,[§] Adri C. T. van Duin,[⊥] Franz-Josef Ulm,[‡] and Roland J.-M. Pellenq[‡],[∥]

[‡]Concrete Sustainability Hub, Department of Civil and Environmental Engineering, Massachusetts Institute of Technology, 77 Massachusetts Avenue, Cambridge, Massachusetts 02139, United States
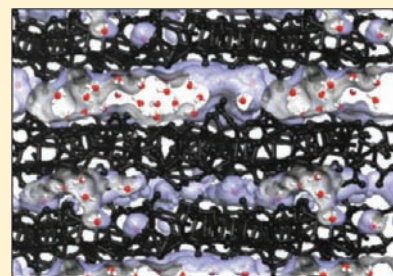
[§]Physique des Interactions Ioniques et Moléculaires (UMR6633), Université de Provence, Avenue Escadrille Normandie-Niemen-Saint Jérôme, Case 242, 13397 Marseille Cedex 20, France

[⊥]Department of Mechanical and Nuclear Engineering, Pennsylvania State University, University Park, Pennsylvania 16802, United States

[∥]Centre Interdisciplinaire des Nanosciences de Marseille, Centre National de la Recherche Scientifique and Marseille Universite, Campus de Luminy, 13288 Marseille Cedex 09, France

S *Supporting Information*

ABSTRACT: Interest in microporous materials has risen in recent years, as they offer a confined environment that is optimal to enhance chemical reactions. Calcium silicate hydrate (C-S-H) gel, the main component of cement, presents a layered structure with sub-nanometer-size disordered pores filled with water and cations. The size of the pores and the hydrophilicity of the environment make C-S-H gel an excellent system to study the possibility of confined water reactions. To investigate it, we have performed molecular dynamics simulations using the ReaxFF force field. The results show that water does dissociate to form hydroxyl groups. We have analyzed the water dissociation mechanism, as well as the changes in the structure and water affinity of the C-S-H matrix and water polarization, comparing the results with the behavior of water in a defective zeolite. Finally, we establish a relationship between water dissociation in C-S-H gel and the increase of hardness due to a transformation from a two- to a three-dimensional structure.

INTRODUCTION

Ultraconfined environments such as zeolites, metal−organic frameworks, and microporous carbon have received a lot of attention from the scientific community owing to their applications as, for example, hydrogen storage compounds or catalysts.[1,2] Of special interest is the behavior of water in such extreme conditions. Due to the constrained geometry, water exhibits unique properties far different from those in the bulk state, including a shift of the dipolar moment,[3] ice-like immobilization,[4] higher heat capacity,[5] and anomalous molecular rotations.[6] However, the dissociation of water in micropores and the impact of these chemical reactions on the materials' properties have not been studied so far, to the authors' knowledge. Micropores might be a perfect environment for water dissociation, as they have proven to enhance chemical reactions.[1] From the atomistic simulation point of view, *ab initio* methods can be used to study chemical reactions at materials interfaces with great accuracy,[7,8] yet the large number of atoms and especially the time necessary to observe chemical reactions make them impractical in many situations. Reactive Monte Carlo (RxMC) methods have been used to study the reaction of small molecules such as formaldehyde, NO, and propene in confined environments, overcoming the system size problem.[9−11] However, the development of reactive force

fields[12−14] opens the opportunity to investigate chemical reactions using fast empirical potentials, without any *a priori* information about the system. The reactive force field employed in this work, ReaxFF, has already shown its ability to reproduce chemical reactions in confined geometries, such as *n*-propyl radical formation in Mo_3VO_x nanochannels.[15] The main objective of this work is to study water dissociation in confined micropores, and its effect on their structure and properties, using as a model system calcium silicate hydrate (C-S-H) gel.

C-S-H gel is the main constituent of cement-based materials. It is the phase which glues the multiple crystalline hydrates, gives cohesion to the material, and is mainly responsible for cement's strength.[16] Broadly defined, C-S-H gel is a disordered material composed of short silicate chains held together by calcium oxide regions, with water trapped inside the structure.[17,18] As can be seen in Figure 1, the interlaminar space in C-S-H gel, with an average distance of a few angstroms, is a likely environment for water dissociation. In fact, a recent work using molecular dynamics (MD) has found that the inter-laminar space is a highly hydrophilic region, where the silicate
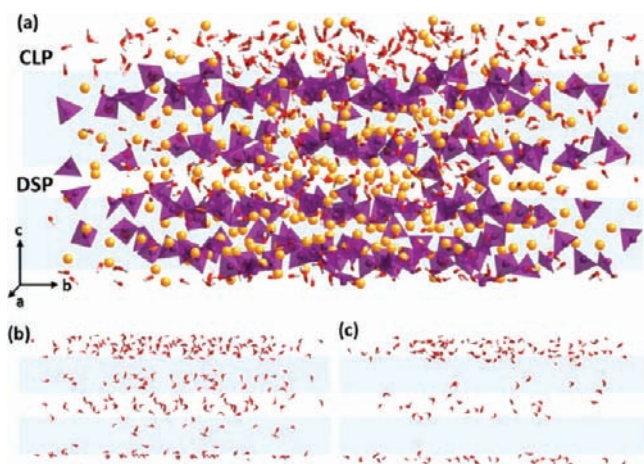
Figure 1. (a) Atomic representation of the C-S-H molecular model. The silicate groups (SiO_4^{4-}) are represented as blue tetrahedra, the calcium atoms as orange spheres, and the water molecules/hydroxyl groups as red and white jointed sticks. Below it the water molecules are represented alone from the model before (b) and after (c) dissociation reactions. The decrease in the number of water molecules can be easily appreciated. The blue regions remark the calcium silicate layers for a better visual comparison of the substrate. The two different pore spaces (CLP and DSP) are also indicated.

Figure 2. Pore space representation on C-S-H gel and silicalite structures computed using the Connolly surface method. The inner and outer parts of the pore are in white and blue, respectively, and all the frame atoms are in black for a better view of the pore space.

oxygen atoms are strong hydrogen bond acceptors.[19] C-S-H gel is therefore a convenient system to test the effect of water dissociation. Furthermore, under such conditions, the extra degree of freedom of the chemical reaction might give us a better understanding of the material's properties, which are of great technological and industrial interest.[20]

COMPUTATIONAL METHODS

In order to study the possible chemical reactions in the C-S-H model, we have performed reactive MD simulations with the ReaxFF force field. ReaxFF uses a bond length–bond order scheme to describe atomic interactions allowing chemical bond to break and form. ReaxFF has been successfully applied to the study of many chemical systems, such as hydrocarbons, water–oxide interfaces, and catalytic processes in nanoparticles.[13,21,22] We extended the ReaxFF capabilities to integrate calcium interactions (Ca−O−H) with the previously developed Si−O−H set,[23] so reactive MD of calcium silicates can now be performed. Details about the force field parametrization and performance will be published elsewhere.[24]

All C-S-H gel simulations were performed in a 3×1×1 supercell of the model constructed by Pellenq et al.,[25] and the lattice parameters before the MD simulations are specified in Table 1. For comparison of some results, several simulations have been carried out in silicalite-1 zeolite. Its structure consists in an orthorhombic unit cell with interconnected channels running in the [001] and [010] directions.[26] In both cases, the initial amount of water absorbed within the structure was determined using Grand Canonical Monte Carlo simulations, by equilibrating the system with a reservoir of liquid water ($P/P_o = 1$). Hence, the water content was determined directly from atomistic simulation without any assumption. We refer the reader interested in more details about the water absorption to refs 3 and 25.

We performed MD with the LAMMPS code,[27] using a Verlet algorithm to integrate the trajectories, and a time step of 0.25 fs. The first run was for 250 ps in the canonical ensemble at 298 K, with a Nosé-Hoover thermostat and coupling constant of 100 fs. After 250 ps equilibration, we moved to the isothermal−isobaric ensemble at room conditions ($T = 298$ K and $P = 1$ atm) until the energy and the lattice parameters converged (4 ns of simulation). We continued the simulation up to 4.5 ns to average the properties during the last 250 ps. The elastic t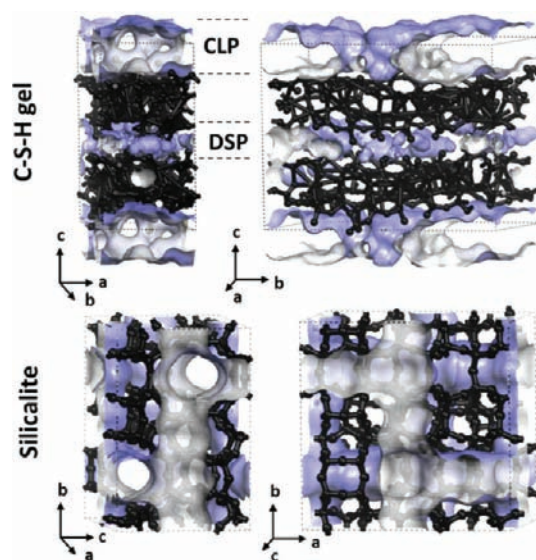ensor and the hardness of the C-S-H structure were computed through strain−stress relationships. For the elastic tensor, the strain was applied in steps of 0.5%, both expansion and compression, and the atomic positions relaxed by a conjugate gradient energy minimization at 0 K. For the hardness, the stress−strain curve was computed applying shear strain in the xz direction in small steps of 0.05%, relaxing the atomic positions after each deformation using a conjugate gradient minimizer.

DFT calculations were done with the Siesta code.[29] SIESTA uses a linear combinations of atomic orbitals to describe valence electrons, together with a nonlocal norm-conserving Troullier−Martins pseudopotential[30] that is factorized in the Kleinman−Bylander form[31] to account for atomic cores. In the present calculation, the exchange and correlation local density approximation (LDA) proposed by Ceperley and Alder[32] is used, with a double-zeta polarized (DZP) basis sets for all atoms. The structural minimization using a conjugate gradient algorithm was stopped when the maximum force component at each atom was smaller than 0.04 eV/atom. The forces were computed using a variant of the Helman−Feynman theorem which includes Pulay-like corrections[33] to account for the fact that the basis sets are not complete. The simulations were done using the gamma point and a grid cutoff in real space of 50 Ry.

RESULTS AND DISCUSSION

Pore Structure of the Studied Systems. A characterization and explanation of the pore structure is necessary for a clear discussion of the results. We have measure the pore volume in both C-S-H gel and silicalite using the "Connolly surface" method.[34,35] We considered a characteristic water radius of 1.4 Å for the test particle, and van der Waals radii of 2.1, 1.97, and 1.52 Å for Si, Ca, and O, respectively. For silicalite, the total porosity of 1566.5 Å³ per unit cell equivalent to a 31% of its volume. This results are in agreement with those reported previously for this zeolite,[36] validating our computation of the pore space structure. For the C-S-H, the water-accessible volume before water dissociation is 24% (5537.4 Å³/unit cell), with an irregular pore size due to its disordered morphology. An important distinction must be made between the two main interlayer regions, which present very dissimilar pore structures. The first one forms a two-dimensional channel of radius ∼7.5 Å running perpendicular to the [001] direction. The second
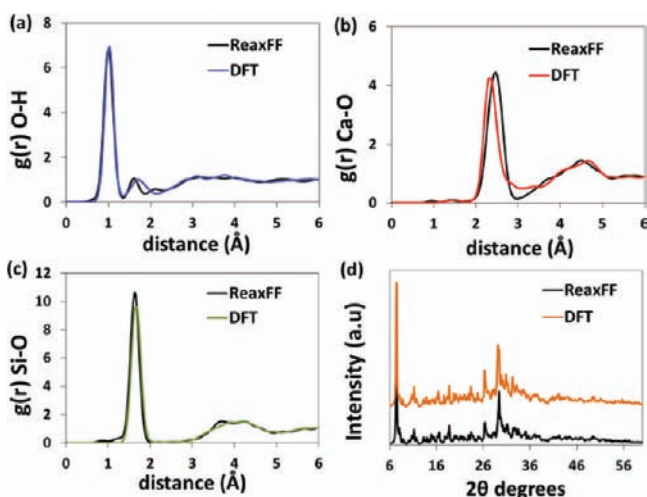
Figure 3. (a−c) Computed radial pair distribution functions of the O−H, Ca−O, and Si−O pairs from the relaxed ReaxFF and DFT configurations. Note the lack of long-range order despite the $g(r)$ where computed only at the equilibrium configuration, which clearly corroborates the glassy nature of the C-S-H substrate. (d) X-ray diffraction pattern of the relaxed ReaxFF and DFT configurations. The computations were done using the Mercury Code,[28] with a Cu Kα radiation wavelength and a broadening of 0.2 Å.

interlaminar region is only connected in the [100] direction, and several pockets accessible in size to water are present. For simplicity in the discussion, we will refer to the two pore regions in the rest of the text as connected large pore (CLP) and disconnected small pore (DSP) (see Figure 2). It must be noted that, due to the disorder, adjacent layers are connected by ionic bonds, which in terms of accessible volume for water creates a three-dimensional structure rather than independent layers.

Water Dissociation Mechanism. First, geometry optimization was carried at 0 K out to check the stability of the C-S-H model developed by Pellenq et al.,[25] using both ReaxFF and DFT simulations. The simulations converged, and just small atomic displacements were found, without big rearrangements. We compare in Figure 3 the radial pair distribution functions $g(r)_{X-O}$, where X = Ca, Si, and H, of the relaxed ReaxFF and DFT configurations. The $g(r)_{X-O}$ do not show any substantial difference, with a great agreement in the first peaks and slightly more defined secondary peaks for the ReaxFF simulations. The X-ray diffraction patterns of the relaxed structures are also included in Figure 3, showing excellent agreement between DFT and ReaxFF, and using these together with the $g(r)$, we can assess the reliability of our reactive force field and the stability of the C-S-H molecular model.

It is interesting to note that no water molecules dissociated during 0 K energy minimization in either simulation. However, when we moved to the canonical ensemble ReaxFF MD simulation at 300 K, we observed water molecules dissociating to form Si−OH and Ca−OH groups. Each water molecule dissociation produces a OH⁻−H⁺ ionic pair. The H⁺ atom then moves to the nonbonding silicate oxygenatom of the silicate chains, while the remaining OH⁻ group will be coordinated to the interlaminar Ca²⁺ ions. A clear distinction can be made between the reactivity of bridging silicate oxygen (BO) and NBO atoms, namely those that link two silicon atoms and those that are coordinated to calcium. In our simulation, all the dissociated water molecules react with the NBO atoms. It is

well known from other microporous silicates that siloxane oxygen atoms exhibit a hydrophobic behavior.[37] It is not surprising then that none of these oxygen atoms reacted with water, while the NBO oxygen atoms reacted to become silanol groups. As a matter of fact, a relationship between the amount of NBO atoms and the number of hydroxyl groups has been found in silicate glasses following the band intensities in microRaman spectrometry.[38,39] Regarding the effect of the Ca²⁺ counterions, we expect the same mechanism to be general for any cation, the dissociation being slower or faster depending on their electronegativity. This model will be corroborated in a future work, using different cations such as Mg²⁺ or Na⁺ to replace Ca²⁺.

The dissociation is a fast process that occurs within the first 0.2 ns of simulation (see Figure 4a). The quickness of the reactions compares well with previous simulation of water dissociation at the surface of amorphous silicate glasses.[23] The high hydrophilicity of some atomic sites found in the C-S-H model was in fact an indication of their high reactivity.[19] After 0.2 ns, as much as 44% of the water molecules have dissociated to form Si−OH and Ca−OH bonds. The rest of the water molecules remain in a molecular form during the remaining simulation time. Dissociative water is therefore likely to be a constitutive part of C-S-H gel, as several experimental studies and models suggest.[18,40,41] It is worth mentioning that no other reactive event was detected during the 4.5 ns of simulation. In particular, the silicate monomers present in the system did not react to form longer chains. This reactions were expressly followed due to the large amount of silicate monomers in the C-S-H model, about 3 times the amount determined by ²⁹Si and ¹⁷O cross-polarized NMR.[42,43] From our simulation we can conclude that, if monomers get trapped within C-S-H gel during the nucleation process, they might remain stable. This finding is in agreement with experimental results, which detect about 3% of silicate monomers in cement pastes after 80% hydration at room temperature, and that might increase to 8% at 343 K.[42,43] A plot of the Qn silicate sites percentage evolution during the simulation can be seen in Figure 4b. The %Qn is constant, showing the stability of the silicate sites.

We have analyzed the atomic density of water and hydroxyl molecules in the ab plane of C-S-H gel after water dissociation (Figure 5). Due to the dissimilar pore structure, water was irregularly distributed, with almost double the amount of water in the CLP. After the water dissociation reactions, we observe that in the CLP about 75% of water remains stable, and the pore thickness is kept. However, approximately 60% of the water in the SDP has dissociated, and the pore diameter has decreased about 1 Å.

Water Properties and Hydrophilicity of the Substrate. To study of the hydrophilic−hydrophobic character of C-S-H gel and the possible changes after dissociation reactions, we analyze the dipolar moment distribution of the water molecules and compare it with that of bulk water. The dipolar moment distribution was computed following the method described in ref 23. ReaxFF uses a charge equilibration method that imposes electroneutrality to the simulation cell, but not to every independent molecule. Hence, water molecules may not be electroneutral in certain steps. To overcome this problem, the dipolar moment was computed, splitting the charge of the oxygen atom into the two hydrogen atoms, ensuring molecular electroneutrality. The dipolar moment can differ from one molecule to another and over MD steps due to the variation of the oxygen atom charge and the geometry of the water
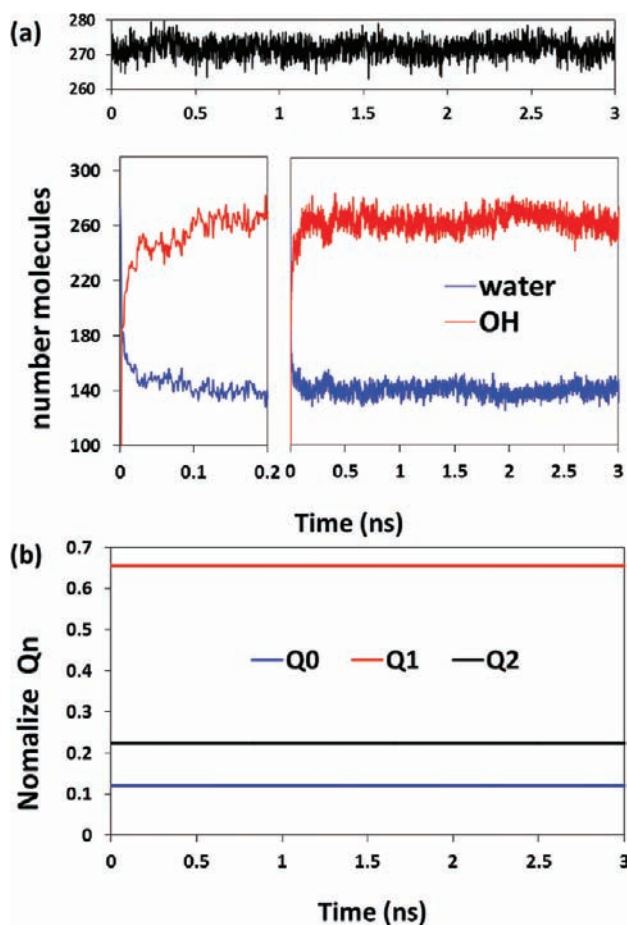
Figure 4. (a) Water and OH evolution during the simulation time, in blue and red, respectively. The upper graph shows the sum of both water and hydroxyl groups. (b) Evolution of the silicate groups' connectivity with time. The Qn nomenclature, common in ^{29}Si NMR, represents the number of silicate groups linked to the given one through siloxane bonds. Q0 represents an isolated silicate group, Q1 represents a silicate group at the end of a chain, and Q2 represents a silicate group in an internal position.

Figure 5. Molecular density in the plane parallel to the silicate layers (c direction). The blue and black lines represent the center of mass of the water and OH groups, respectively, and the red dashed line represents the water molecules before dissociation. The red shadows symbolize the solid calcium silicate region.

molecule, being fully flexible in ReaxFF. The results are presented in Figure 6a. The value for bulk water is 2.07 D, below the experimental value of 2.9 D. The low dipolar moment of bulk water compared to those obtained with other force fields, such as SPC or TIP3P,[44] might arise from the lower atomic charges computed with the Qeq method, about 0.1 e[−] less than in the mentioned models.

In C-S-H gel the dipolar moment is shifted toward higher values by 11% (2.33 D), in good agreement with the trend observed by Youssef et al.[19] for the undissociated state. Using a SPC water model, they demonstrated that the calcium silicate substrate was a hydrophilic environment, hence the shift of water dipolar moment toward higher values. For comparison and discussion, we have computed the dipolar moment distribution of water confined in the hydrophobic zeolite silicalite.[45] Using Hartree−Fock simulations, the dipole distribution was shown to decrease with respect to bulk water.[46] Our ReaxFF MD simulation is in good agreement, as we observe the same dipolar moment shift toward lower values. However, we have introduced a defective site in the silicate network to create NBO atoms analogous to those of C-S-H gel. The defect consisted of a vacant silicon atom, generating four ending oxygen atoms, and two calcium ions for electroneutrality.
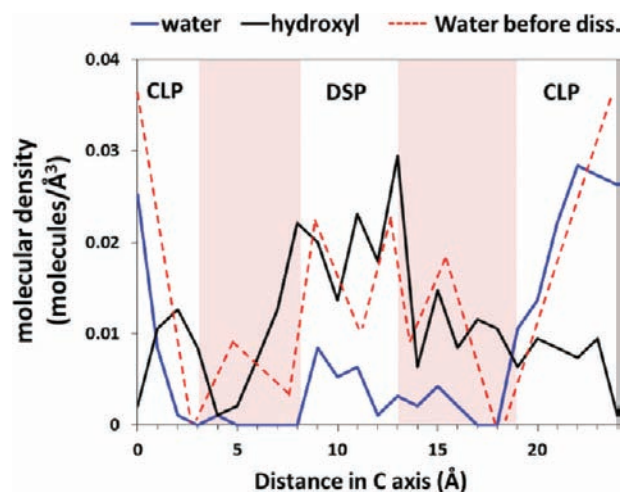
During the MD simulation, we observed water dissociation in the terminal oxygen atoms, the same process as in C-S-H gel. The impact on the dipolar moment can be seen in Figure 6b: the curve is still shifted toward lower dipolar moments with respect to pure water, but there is a shoulder at higher dipolar moments. The shoulder is a consequence of the polarization induced by the defect and the counterions, and similar contributions have been found in substituted LTA zeolites.[37] In the zeolite, the defective area causes just a perturbation in the otherwise hydrophobic environment, and hence it is manifested as a shoulder in the dipole distribution, while the disorder C-S-H structure has many defective areas (ending oxygen atoms of the silicate chains) that shift the entire dipole distribution. It must be mentioned that the three-dimensional zeolite network was not affected by the presence of the defect, keeping intact its structure.

The water density can also give us an indication of the substrate affinity toward water. While in silicalite the value is about half of the bulk water density,[36] in the C-S-H it is as high as 1.47 g cm^{−3}. After the chemical reactions, both the pore volume and the molecular water content decrease, giving a final density of 1.31 g cm^{−3}. This value should be taken as a qualitative measurement, due to the uncertainty in the pore volume computation and the fact that the structural water trapped inside the isolated pockets of the DSP was taken into account for the density computation. Nevertheless, the number depicts the hydrophilicity of the substrate.

After studying the amount of reacted water and the places where the reactions took place, we analyzed the structure of the remaining water molecules. The O−H bonds are split into a bimodal distribution before water dissociation. The main peak at 0.98 Å agrees with the equilibrium distance computed by ReaxFF,[23] while the second peak corresponds to a bond stretch due to the strong hydrogen-bonding between the water molecules and the hydrophilic substrate (see Figure 7). After the reactions, the O−H distances of the water molecules lose the bimodal distribution and are spread around a value of 1.02 Å. The wide bond length distribution might be associated with a higher disorder generated after water dissociation in the calcium silicate skeleton, as we will discuss later. A wider
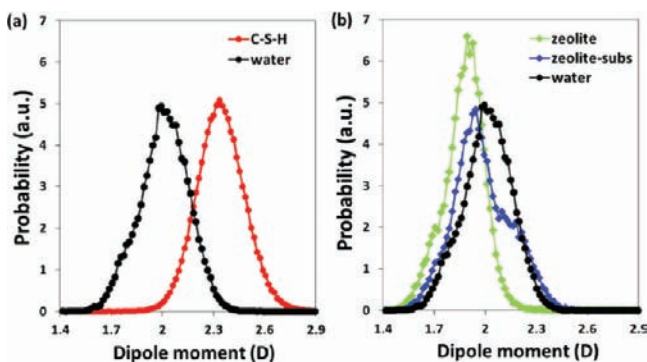
Figure 6. Dipolar moment distribution (in debye) of the water molecules in bulk water (black dots and line) and in the C-S-H (red). The shift toward higher values is a hallmark of the C-S-H hydrophilicity. (b) For comparison with the previous, dipolar moment distribution (in debye) of the water molecules in bulk water (black), in a zeolite (green), and in a defective zeolite (blue). The shoulder shows how the usual hydrophobic character is modified by the presence of defects.

scattering after dissociation is also found in the H−O−H angle distribution, centered on 102.5°, slightly smaller than the ReaxFF value for bulk water (104.5°),[23] probably due to the disorder and confinement of the water molecules.

Impact of Water Dissociation on the C-S-H Structural Order. After 250 ps, when all the reactions had taken place, we moved to the isothermal−isobaric ensemble at room conditions (T = 298K and P = 1 atm) and analyzed the volumetric changes of C-S-H gel due to the water dissociation. In Table 1 we present the final structural parameters averaged over the last 0.25 ns of simulation. The overall volume of the system decreased 4.7%, increasing the density from 2.45 to 2.57 g/cm³, closer to the experimental value of 2.6 g/cm³ obtained from SANS.[18]

The arrangement structure within the unit cell was analyzed by computing the radial pair distribution functions $g(r)$ and the X-ray powder diffraction patterns. The data were averaged during the last 0.25 ns of simulation in both cases. We can see in Figure 8 that the $g(r)$ does not change much with respect to the relaxed structure. The first peaks are slightly narrowed, the Ca−O distances have decreased ∼0.04 Å, and the O−H radial distribution is more disordered after the first peak. The great match shows that, despite the hydroxyl formation, the atomic environment is kept. The shape of the peaks clearly corresponds to a material with glass-like structure, with short-range order that vanishes at longer distances. Similarly, no significant differences were found in the X-ray diffraction pattern, just a lower intensity of the peaks in the region around 30°. The spectrum illustrates an increase of the long-range disorder in the C-S-H model due to the formation of hydroxyl groups: the dissociation of water introduces a new degree of freedom that modifies the energy landscape of the structure, allowing further relaxation toward a more disordered and energetically favorable configuration. The order/disorder of C-S-H gel at short distances is still a controversial topic,[17] though this and previous atomistic simulation studies show that disordered particles can reproduce the experimental structure, densities, and mechanical properties.[25,40,47]

Impact of Water Dissociation on the C-S-H Mechanical Properties. Finally, the elastic properties of the simulated C-S-H structure have been computed. In Table 2 we present
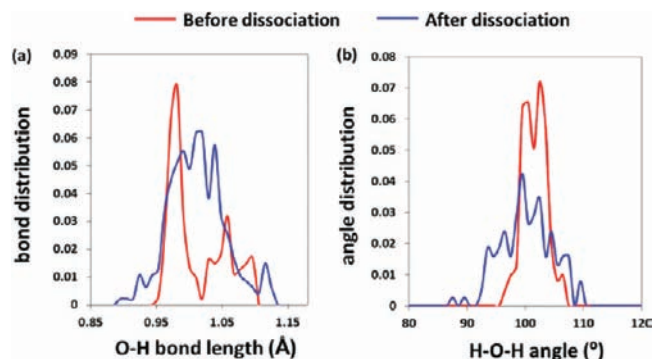

Figure 7. (a) O−H bond length distribution and (b) H−O−H angle distribution of the water molecules in the C-S-H model before (red lines) and after (blue lines) water dissociation.

Table 1. Structural Parameters of the C-S-H Model after Water Dissociation Reactions[a]

a (Å)	39.45 (39.93)	α (deg)	93.35 (92.02)
b (Å)	28.79 (29.52)	β (deg)	84.54 (88.52)
c (Å)	24.16 (23.69)	γ (deg)	126.40 (123.58)
V (nm³)	21.98 (23.07)	ρ (g/cm³)	2.57 (2.45)
composition		$C_{1.65}SH_{0.77} \cdot 0.98H_2O$ ($C_{1.65}SH_{1.75}$)	

[a]The results are averaged over 0.25 ns of MD simulation at room temperature and pressure. The values in parentheses are those before water reactions.

the full elastic tensor and the elastic properties derived from it. We can compare our simulations with the experiments through the indentation modulus, M, particularly accessible from nanoindentation measurements. Our simulation predicts 69 GPa, in very good agreement with the nanoindentation result of 65 GPa.[48] The change in elastic properties is almost negligible with respect to the original C-S-H model with unreacted water.[25] We can conclude that the presence of the hydroxyl group does not affect importantly the elastic properties of the C-S-H structure. Furthermore, the results suggest that elastic properties are mainly driven by the glassy nature of the model, in contrast with the higher dependence on the water/hydroxyl content reported for hydrated calcium silicate crystals.[47,49]

Conversely, the shear stress versus shear strain behavior before and after water dissociation has some important differences. In Figure 9a we present the shear stress plotted against the shear strain for the C-S-H model before and after water dissociation in red and blue respectively. The profile is the same in both cases, showing an initial increase of the stress interspersed with small drops due to local stress relaxation. After reaching a maximum stress, the drops are more significant entering pseudo-plateau of stress accumulation and relaxation. There is an important increase in the maximum stress before and after water dissociation, from 2.25 to 3.75 GPa. The underlying relaxation mechanism can be understood by looking at the atomic displacement during a relaxation step in one of the stress drops in Figure 9b,c. Before dissociation, the relaxation involves the entire unit cell, mainly focalized in the water region. After dissociation reactions, there is a clear localization of the atoms involved in the relaxation in the big pore area. The difference could be explained by the flexibility of that water molecules introduce in the structure, acting as a lubricant between the solid calcium silicate frame and allowing atomic displacement to relax the stress. When water dissociates,
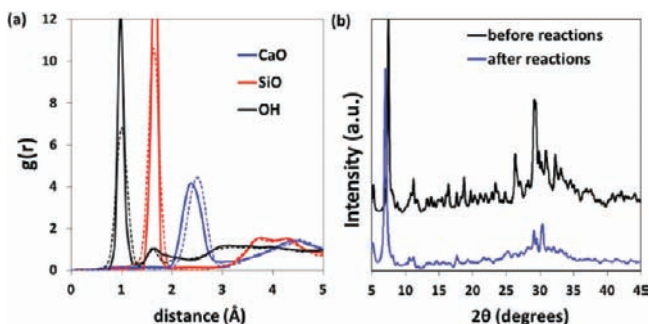
Figure 8. (a) Radial pair distribution functions $g(r)$ for the Ca−O, Si−O, and H−O pairs before dissociation (dashed lines) and after dissociation (full lines). (b) Computed X-ray diffraction pattern for the C-S-H model before and after water dissociation, with the same conditions as described in Figure 1.
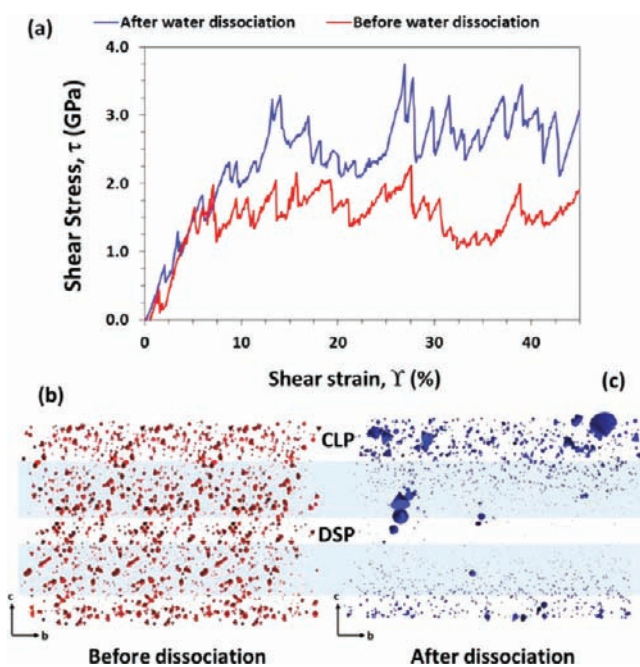
Table 2. Elastic Tensor Coefficients of the C-S-H Model after Water Dissociation and the Derived Elastic Properties[a]

C_{ij}	1	2	3	4	5	6
1	90.9	33.1	30.0	−1.9	0.3	−1.2
2		91.7	29.6	0.1	0.4	0.6
3			72.6	−0.3	0.0	0.0
4				21.4	0.3	0.2
5					21.0	0.3
6						28.6
			Elastic Properties			
K_H	48.6(49)	G_H	24.7(23)	M	69.0(65)	
E_x	72.8(66)	E_y	74.0(68)	E_z	58.3(55)	
E_{ani}	63.5	η	0.28(0.3)			

[a]All the values are presented in GPa. The bulk (K) and shear (G) moduli are presented in the Hill definition,[50] and the polycrystalline Young modulus (E_{ani}), Poisson ratio (η), and indentation modulus (M) are computed from them.

Figure 9. (a) Shear strain versus shear stress curves in the xz direction, i.e., parallel to the silicate chains, before and after water dissociation. (b,c) Displacement of the atoms in the C-S-H structure after the first significant drop in the shear stress (8% strain for the system before dissociation reactions and 14% strain after). The size of the arrows represents the magnitude of the displacement. All the atoms have been removed for a better view, and the solid frame regions are showed in blue as in previous figures. The displacements were computed using the OVITO code.[51].
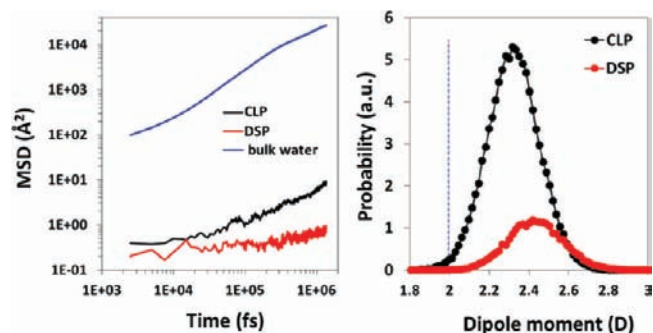

Figure 10. (a) Mean square displacement of the water molecules in bulk water, connected big pore (CLP), and disconnected small pore (DSP). (b) Dipolar moment distribution in the CLP and DSP. The dashed blue line represents the mean dipolar moment for bulk water obtained by ReaxFF, taken from the distribution in Figure 6.

must considered structural water. Note that the term "ice-like" refers here to the dynamic behavior of the molecules, and they do not present any structural order. The dipolar moment distribution of the water molecules is slightly higher in the DSP than the one in the CLP, which indicates stronger interaction with the substrate. We can claim that the water dissociation in the DSP has decrease the pore volume, so the unreacted water is not diffusive at all, forming part of the frame as structural water, so it does not act as a lubricant for the shear relaxation. Two movies with the atomic configuration during the shear strain are included in the Supporting Information to illustrate this discussion.

An interesting conclusion can be extracted comparing this behavior with other materials. It is clear that the presence of water in the C-S-H is intimately connected to the material hardness. Similar effect, called "hydrolytic weakening" has long time identified in silicates.[52,53] However, the weakening mechanism is dissimilar. In silicates, it is suggested that the water decreases the strength when attacks the siloxane bonds and dissociates, creating Si vacancies populated by hydrogen.[54,55] Conversely, water decreases the strength in C-S-H gel *until* it reacts with the silicate chains. The key point, then, might not be the hydroxilation degree of the silicate units but the connectivity of the whole structure. When water reacts in quartz it breaks chemical bonds and causes discontinuities in the three-dimensional covalent bond network. When water reacts in

especially in the DSP, the structure becomes more rigid and can accumulate more stress before the relaxation steps, still governed by the remaining water of the big pore.

For further evaluation of this effect, we have computed separately the mean square displacement (MSD) and dipolar moment distribution of the water molecules in the big and small pores, shown in Figure 10. The big pore already shows the smaller water diffusivity than bulk water characteristic of confinement, but the MSD decrease in the small pore is dramatic. In 1.4 ns, the displacement of the water molecules is confined to less than 1 Å^2, which suggest an ice-like behavior of water in in this very small pockets or close pores, and hence it

C-S-H gel the interlaminar space decreases, evolving from a two-dimensional layered structure to a three-dimensional glass. Hence, we can conclude that the shear strength is influenced by the three-dimensional connectivity rather than a particular water-hydroxyl state.

CONCLUSION

In this work we have studied by atomistic simulation the dissociation and polarization of water in the micropores of the calcium silicate hydrate (C-S-H) gel. Using a reactive force field (ReaxFF) we have analyzed the chemical reaction mechanism and the implications on the structure and mechanical properties of the material.

A considerable amount of the water present in C-S-H gel pore space dissociates to form Ca−OH and Si−OH groups. All the water reacts in the NBO atoms of the silicate chains forming silanol groups, while none of the siloxane oxygen atoms reacts. The water affinity to the substrate does not change after the chemical reactions. Before water dissociation, the solid C-S-H was hydrophilic, due to the strong acceptor character of the silicate chain terminal oxygen atoms. The new silanol groups keep the hydrophilic character of the solid part, as can be inferred from the water dipolar moment distribution. We compare this result with a defective zeolite structure with a silicon vacancy counterbalanced by calcium atoms. Similarly to the C-S-H, water dissociates forming silanol groups around the defect and creating a hydrophilic area than can be appreciated as a shoulder in the dipolar moment distribution. In general, we can suggest that NBO atoms in silicate structures have a hydrophilic character while siloxane oxygen atoms have a hydrophobic character.

The water dissociation reactions do not affect much the short-range order and elastic properties of C-S-H gel, yet there is a greater impact on its shear strength. We identified the lubricant effect of the water molecules as the stress relaxation mechanism. After dissociation, the water in the DSP presents an ice-like behavior, and hence does not contribute to the relaxation, leading to a hydraulic increase of the C-S-H shear strength. This effect is contrary to the hydrolytic weakening in silicates, were the water dissociation leads to a decrease on the elastic properties. We can suggest that the disruption of the three-dimensional iono-covalent bonding network is the main reason of the strength decrease, and water dissociation can affect in both directions, i.e. increasing or decreasing the three-dimensional connectivity at the atomic scale.

Overall we propose a model that will describe the general hydroxylation process in micropores of defective silicates like zeolites or amorphous silicate glasses, as well as the impact of such dissociation in the stiffness of the substrate. This is the first study on the water dissociation in confined environments, and we show the great importance of account for chemical reactions for a better understanding and description of materials properties. Our work also opens the possibility of investigating the impact of pressure and temperature on the water dissociation, parameters of great interest in geological research.[56]

ASSOCIATED CONTENT

Ⓢ Supporting Information

Shear stress−strain relaxation movies before and after water dissociation. This material is available free of charge via the Internet at http://pubs.acs.org.

AUTHOR INFORMATION

Corresponding Author

hegoi.manzano@ehu.es

Present Address

†Dpto. Química Física, Universidad del País Vasco (UPV/EHU), Aptdo. 644, 48080 Bilbao, Spain

REFERENCES

(1) Lu, G.; Zhao, X. S. In *Nanoporous materials: science and engineering*; Lu, G. Q., Zhao, X. S., Eds.; Imperial College Press: London, 2004.

(2) Lísal, M.; Brennan, J. K.; Smith, W. R. *J. Chem. Phys.* **2006**, *124*, 064712.

(3) Puibasset, J. l.; Pellenq, R. J. M. *J. Phys. Chem. B* **2008**, *112*, 6390−6397.

(4) Mashl, R. J.; Joseph, S.; Aluru, N. R.; Jakobsson, E. *Nano Lett.* **2003**, *3*, 589−592.

(5) Tombari, E.; Salvetti, G.; Ferrari, C.; Johari, G. *J. Chem. Phys.* **2005**, *122*, 104712.

(6) Frunza, L.; Kosslick, H.; Pitsch, I.; Frunza, S.; Schönhals, A. *J. Phys. Chem. B* **2005**, *109*, 9154−9159.

(7) Cicero, G.; Grossman, J. C.; Catellani, A.; Galli, G. *J. Am. Chem. Soc.* **2005**, *127*, 6830−6835.

(8) Carrasco, J.; Illas, F.; Lopez, N. *Phys. Rev. Lett.* **2008**, *100*, 4.

(9) Johnson, J. K.; Panagiotopoulos, A. Z.; Gubbins, K. E. *Mol. Phys.* **1994**, *81*, 717−733.

(10) Santiso, E. E.; George, A. M.; Turner, C. H.; Kostov, M. K.; Gubbins, K. E.; Buongiorno-Nardelli, M.; Sliwinska-Bartkowiak, M. G. *Appl. Surf. Sci.* **2005**, *252*, 766−777.

(11) Hansen, N. *J. Chem. Phys.* **2005**, *122*, 164705.

(12) Brenner, D. W.; Shenderova, O. A.; Harrison, J. A.; Stuart, S. J.; Ni, B.; Sinnott, S. B. *J. Phys.: Condens. Matter* **2002**, *14*, 783−802.

(13) van Duin, A. C. T.; Dasgupta, S.; Lorant, F.; Goddard, W. A. *J. Phys. Chem. A* **2001**, *105*, 9396−9409.

(14) Mahadevan, T. S.; Garofalini, S. H. *J. Phys. Chem. B* **2007**, *111*, 8919−8927.

(15) Chenoweth, K.; van Duin, A. C. T.; Goddard, W. A. *Angew. Chem., Int. Ed.* **2009**, *121*, 7766−7770.

(16) Taylor, H. F. *Cement Chemistry*, 2nd ed.; Thomas Telford Publishing: London, 1997.

(17) Skinner, L. B.; Chae, S. R.; Benmore, C. J.; Wenk, H. R.; Monteiro, P. J. M. *Phys. Rev. Lett.* **2010**, 104.

(18) Allen, A. J.; Thomas, J. J.; Jennings, H. M. *Nat. Mater.* **2007**, *6*, 311−316.

(19) Youssef, M.; Pellenq, R. J. M.; Yildiz, B. *J. Am. Chem. Soc.* **2011**, *133*, 2499−2510.

(20) SchneiderM.RomerM.TschudinM.BolioH.Cem. Concr. Res.2011

(21) Raymand, D.; van Duin, A. C. T.; Spangberg, D.; Goddard, W. A.; Hermansson, K. *Surf. Sci.* **2010**, *604*, 741−752.

(22) Keith, J. A.; Fantauzzi, D.; Jacob, T.; van Duin, A. C. T. *Phys. Rev. B.* **2010**, *81*.

(23) Fogarty, J. C.; Aktulga, H. M.; Grama, A. Y.; van Duin, A. C. T.; Pandit, S. A. *J. Chem. Phys.* **2010**, *132*, 10.

(24) Manzano, H.; Van Duin, A. C. T.; Ulm, F. J.; Buehler, M. J.; Pellenq, R. J. M. *Langmuir* **2011**, submitted.

(25) Pellenq, R. J. M.; Kushima, A.; Shahsavari, R.; Van Vliet, K. J.; Buehler, M. J.; Yip, S.; Ulm, F. J. *Proc. Natl. Acad. Sci. U.S.A.* **2009**, *106*, 16102−16107.

(26) Flanigen, E. M.; Bennett, J. M.; Grose, R. W.; Cohen, J. P.; Patton, R. L.; Kirchner, R. M.; Smith, J. V. *Nature* **1978**, *271*, 512−516.

(27) Plimpton, S. *J. Comput. Phys.* **1995**, *117*, 1−19.

(28) Macrae, C. F.; Edgington, P. R.; McCabe, P.; Pidcock, E.; Shields, G. P.; Taylor, R.; Towler, M.; van De Streek, J. *J. Appl. Crystallogr.* **2006**, *39*, 453−457.

(29) Artacho, E.; Anglada, E.; Diéguez, O.; Gale, J. D.; Garcia, A.; Junquera, J.; Martin, R. M.; Ordejón, P.; Pruneda, J. M.; Sánchez-Portal, D.; Soler, J. M. *J. Phys.: Condens. Matter* **2008**, *20*, 064208.

(30) Troullier, N.; Martins, J. L. *Phys. Rev. B.* **1991**, *43*, 1993−2006.

(31) Kleinman, L.; Bylander, D. M. *Phys. Rev. Lett.* **1982**, *48*, 1425.

(32) Ceperley, D. M.; Alder, B. J. *Phys. Rev. Lett.* **1980**, *45*, 566.

(33) Pulay, P. *Chem. Phys. Lett.* **1980**, *73*, 393−398.

(34) Gelb, L. D.; Gubbins, K. E. *Langmuir* **1998**, *14*, 2097−2111.

(35) Connolly, M. L. *J. Am. Chem. Soc.* **1985**, *107*, 1118−1124.

(36) Desbiens, N.; Boutin, A.; Demachy, I. *J. Phys. Chem. B* **2005**, *109*, 24071−24076.

(37) Coudert, F. X.; Vuilleumier, R.; Boutin, A. *Chemphyschem* **2006**, *7*, 2464−2467.

(38) Di Muro, A.; Villemant, B.; Montagnac, G.; Scaillet, B.; Reynard, B. *Geochim. Cosmochim. Acta* **2006**, *70*, 2868−2884.

(39) Mysen, B. R. O.; Virgo, D. *Chem. Geol.* **1986**, *57*, 303−331.

(40) Dolado, J. S.; Griebel, M.; Hamaekers, J.; Heber, F. *J. Mater. Chem.* **2011**, *21*, 4445−4449.

(41) Richardson, I. G. *Cem. Concr. Res.* **2004**, *34*, 1733−1777.

(42) Brough, A. R.; Dobson, C. M.; Richardson, I. G.; Groves, G. W. *J. Mater. Sci.* **1994**, *29*, 3926−3940.

(43) Cong, X. D.; Kirkpatrick, R. J. *J. Am. Ceram. Soc.* **1996**, *79*, 1585−1592.

(44) Jorgensen, W. L.; Chandrasekhar, J.; Madura, J. D.; Impey, R. W.; Klein, M. L. *J. Chem. Phys.* **1983**, *79*, 926−935.

(45) Olson, D. H.; Kokotailo, G. T.; Lawton, S. L.; Meier, W. M. *J. Phys. Chem.* **1981**, *85*, 2238−2243.

(46) Pellenq, R.; Roussel, T.; Puibasset, J. *l. Adsorption* **2008**, *14*, 733−742.

(47) Manzano, H.; Gonzalez-Teresa, R.; Dolado, J. S.; Ayuela, A. *Mater. Construcc.* **2010**, *60*, 7−19.

(48) Constantinides, G.; Ulm, F. J. *J. Mech. Phys. Solids* **2007**, *55*, 64−90.

(49) Manzano, H.; Dolado, J. S.; Guerrero, A.; Ayuela, A. *Phys. Status Solidi A-Appl. Mater.* **2007**, *204*, 1775−1780.

(50) Hill, R. P. *Phys. Soc. London A* **1952**, *65*, 349−355.

(51) Stukowski, A. *Modell. Simul. Mater. Sci. Eng.* **2010**, *18*, 015012.

(52) Griggs, D. *Geophys. J. Int.* **1967**, *14*, 19−.

(53) Dingwell, D. B.; Webb, S. L. *Eur. J. Mineral.* **1990**, *2*, 427−449.

(54) Brodholt, J. P.; Refson, K. *J. Geophys. Res.* **2000**, *105*, 18977−18982.

(55) Zhu, T.; Li, J.; Lin, X.; Yip, S. *J. Mech. Phys. Solids* **2005**, *53*, 1597−1623.

(56) Burchard, M.; Maresch, W. V.; Fockenberg, T.; Doltsinis, N. L.; Adeagbo, W. A. *Eur. J. Mineral.* **2011**, *23*, 409−424.